"Investigation of Gas-Sensing Properties of Semiconductor Materials for CO_2 Detection: A Comparative Study of SnO_2, ZnO and Polypyrrole Thin Films"

S. S. Butle, G. T. Lamdhade, K. B. Raulkar, A. O. Chauhan, R. B. Butley, C. C. Jadhao, A. B. More
Department of Physics, Vidya Bharati Mahavidyalaya, Camp, Amravati,
Sant Gadge Baba Amravati University, Amravati, Maharashtra, India.

Abstract: This study investigates the gas-sensing properties of semiconductor materials, specifically tin oxide (SnO_2), zinc oxide (ZnO), and polypyrrole (PPy), for CO_2 detection. The materials were synthesized and characterized using X-ray diffraction (XRD), scanning electron microscopy (SEM), and DC electrical conductivity to evaluate their gas sensing performance. Thin-film sensors were fabricated by mixing SnO_2, ZnO, and PPy in different molar compositions and subjected to CO_2 exposure at various temperatures. XRD analysis revealed the crystallographic structure and crystallite size of the materials, while SEM provided insights into the surface morphology and porosity, key factors in enhancing gas sensitivity. Electrical conductivity and gas sensitivity measurements were carried out to assess the performance of the sensors. Among the different compositions, the sensor with 60% SnO_2 and 40% ZnO (P3) exhibited the highest CO_2 sensitivity, rapid response time, and superior recovery time. Additionally, P3 demonstrated excellent stability and selectivity for CO_2 over other gases like H_2S, LPG, and NH_3. The results suggest that SnO_2-ZnO-PPy composite sensors, especially the P3 variant, can be employed in practical CO_2 gas detection applications due to their superior performance and reliability [1-2].

Keywords: CO_2 gas sensor, Semiconductor metal oxides, (SnO_2), (ZnO), Thin film sensors, Gas sensitivity, Selectivity, Response and recovery time,

1. Introduction

This study focuses on the investigation of gas-sensing properties of semiconductor materials using X-ray diffraction (XRD), scanning electron microscopy (SEM), DC electrical conductivity, and CO_2 gas sensitivity measurements. The main objective is to identify the most suitable sensing material that exhibits high sensitivity, good selectivity, reliable stability, and accurate gas detection performance. Experimental work has been carried out on multilayer thin films of semiconductor oxides exposed to CO_2 gas at different operating temperatures. The materials studied include SnO_2, ZnO, and the conducting polymer polypyrrole (PPy). XRD

analysis is used to study the crystalline structure, while SEM provides information about surface morphology and grain size, which play a crucial role in gas sensing behavior. Electrical conductivity and gas sensitivity measurements help evaluate the sensing performance of each material. It also discusses the growth mechanisms, material characteristics, device applications, and challenges associated with these semiconducting materials for effective CO_2 gas sensing applications [3].

2. Preparation of Materials

The chemicals used for the preparation of Gas Sensor are SnO_2, ZnO, and polypyrrole. Polypyrrole was synthesized by chemical polymerization method in the laboratory. The metal oxide powers were calcinated at 700^0C for 5 hrs. before the use.

2.1 Synthesis of Tin Oxide (SnO_2)

All the chemicals used in this study were of GR grade purchase from Sd-fine, India (purity 99.99%). Stannous chloride dehydrates ($SnCl_2.2H_2O$), Ammonia solution and deionized water were used during reaction. The conducting silver paint (Sigma Aldrich Chemical, USA) is used to form electrodes.

In preparation of SnO_2, 2 g (0.1 M) of stannous chloride dehydrate ($SnCl_2.2H_2O$) is dissolved in 100 ml water. After complete dissolution, about 4 ml ammonia solution is added to above aqueous solution with magnetic stirring. Stirring is continued for 20 minutes. White gel precipitate is immediately formed. It is allowed to settle for 12 hrs. Then it is filtered and washed with water 2-3 times by using deionized water. The obtain precipitate were mixed with 0.27 g carbon black powder (charcoal activated). The obtained mixer is kept in vacuum oven at 70 ℃ for 24 hours so that the mixer gets completely in to dried powder. Then this dry product was crushed into a find powder by grinder. Now obtained product of fine nanopowder of SnO_2 was calcinated at 700^oC up to 6 hours in the auto controlled muffle furnace *(*GAYATRI Scientific, Mumbai, India.*)* so [4] that the impurities from product will be completely removed.

2.2 Synthesis of Zinc Oxide (ZnO)

All the chemicals used in this study were of GR grade purchase from Sd-Fine, India (purity 99.99%). The chemicals are used without any further purification. Zinc acetate dehydrate $Zn(O_2CCH_3)_2(H_2O)_2$, sodium hydroxide, Methanol and deionised water was used during reaction.

In preparation Zinc Oxide (ZnO) 0.2M Zinc Acetate dehydrates was dissolved in 100 ml deionised water was ground for 15 min and then mixed with 0.02 M solution of NaOH with the help of glass rod. After the mixing the solution was kept under constant magnetic stirring for 15 min. and then again it was ground for 30 min. The white precipitate product was formed at the bottom. Then abundant liquid was discarded and the product was washed many times with the deionized water and methanol to remove by products. The final products was then filtered by using wattman filter paper and obtain precipitate in the form of white paste, now this paste was kept in a vacuum oven at 80 ^oC for 4 hrs. So the moisture will removed from the final product and we will get dry product. Then this dry product was crushed into a find powder by using grinding machine and finally this fine nano-powder of ZnO was calcinated at temperature 800 ^oC for 6 hrs. in the auto controlled muffle furnace (Gayatri Scientific, Mumbai, India.) so that the impurities from product will be completely removed and get a final product of ZnO nanoparticles [5].

2.3 Preparation of Polypyrrole

The method used for the preparation of polypyrrole is chemical polymerization. Powder polypyrrole was prepared with 4.290 (high) weight ratio of pyrrole (Py) monomer/oxidant ($FeCl_3$). During the synthesis, concentration of $FeCl_3$ was kept constant and methanol was used as a solvent.

The Py monomer, anhydrous iron (III) chloride ($FeCl_3$) and methanol were used as received for synthesis of PPy. The solution of 7 ml methanol and 1.892 g $FeCl_3$ was first prepared in round bottom flask. Then 8.4 ml Py monomer was added to ($FeCl_3$ + methanol) solution with constant stirring in absence of light. The amount of Py monomer added to the solution (1/2.33 times of $FeCl_3$) was in such a way to get maximum yield.

The polymerization of Py, which was suppressed in a solution, progressed rapidly due to an increase of oxidation potential caused by evaporation of solvent. In the polymerization reaction of Py, it was observed that as soon as the Py monomer was added to the solution, the

colour changed to dark green/black. There was an increase in temperature of the solution during the start of reaction, which showed that it is an exothermic reaction [6]. The reaction was carried out at room temperature for 4 hrs.

The final precipitated polymer was filtered by a conventional method. The polymer was washed with distilled water several times till the filtrate obtained was colourless. To remove last traces of unreacted pyrrole and remaining ferric and ferrous chloride formed due to polymerization, it was then washed with methanol.

The polymer, obtained in powder form was dried first at room temperature for a few hours and then finally dried in an oven (Gallenkamp, British Made) kept at 80^0C for 5-6 hrs. This polypyrrole is then used for active layers of Semiconductor Gas Sensors.

2. Series Preparation

Initially chemicals SnO_2, ZnO (AR grade with 99 % purity) were taken and calcinated at temperature 600^0C to remove the impurity and moisture then inorganically mixed to prepare the sensors. The powder of the chemicals is thoroughly crushed in mortal pestle then mixed in the desire proportion with the help of binder and using screen printing technique, paste is screened out on the thin, clean glass plate. Multi-layers are fabricated and with the help of silver paint, electrodes are produced [7].

The series are prepared to study the response of CO_2 gas sensors. These series are listed in the following figure.

Table 1 Series I of SnO_2-ZnO-PPy

Sr. No.	Sensor codes	Layers
1.	P1	$100SnO_2$/ PPy/GP
2.	P2	$80SnO_2$: 20ZnO/ PPy/GP
3.	**P3**	**$60SnO_2$: 40ZnO/ PPy/GP**
4.	P4	$40SnO_2$: 60ZnO/ PPy/GP
5.	P5	$20SnO_2$: 80ZnO/ PPy/GP
6.	P6	ZnO/ PPy/GP

3. Results and Discussions

3.1 X-ray Diffraction Study

The X-Rays gets diffracted from the reticular planes forming the atoms with in crystal and this phenomenon of diffraction of X-rays is used in XRD. The X-ray after passing through crystal gets diffracted at specific angles. The diffracted beam angles depend on the crystal orientation, structure of the crystal and wavelength of the X-ray. The constructive interference of diffracted rays at a specific wavelength occurs, when the path difference between two diffracted rays from atomic planes surfaces become an integral number of wavelengths. This condition is depicted by the Bragg law [8].

XRD images of pure samples

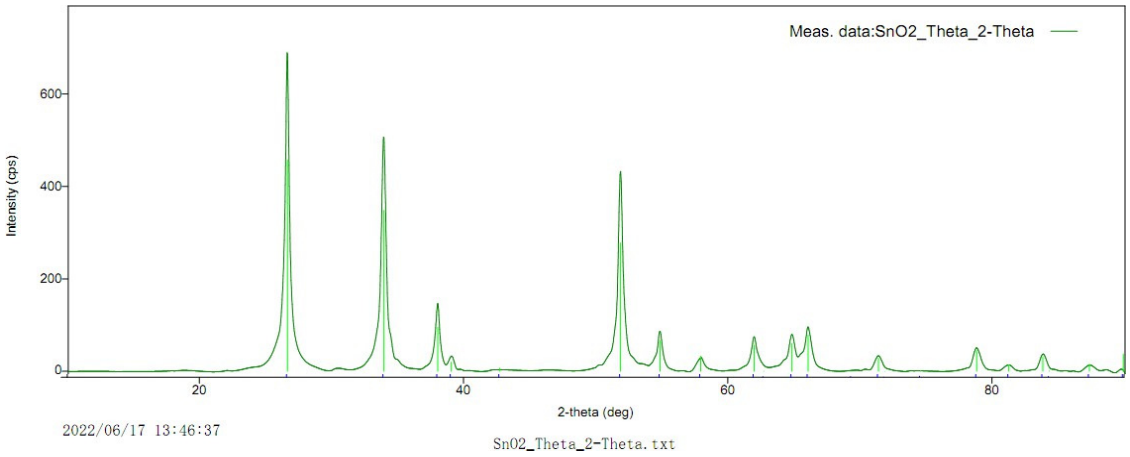

Fig.1 XRD image of SnO_2

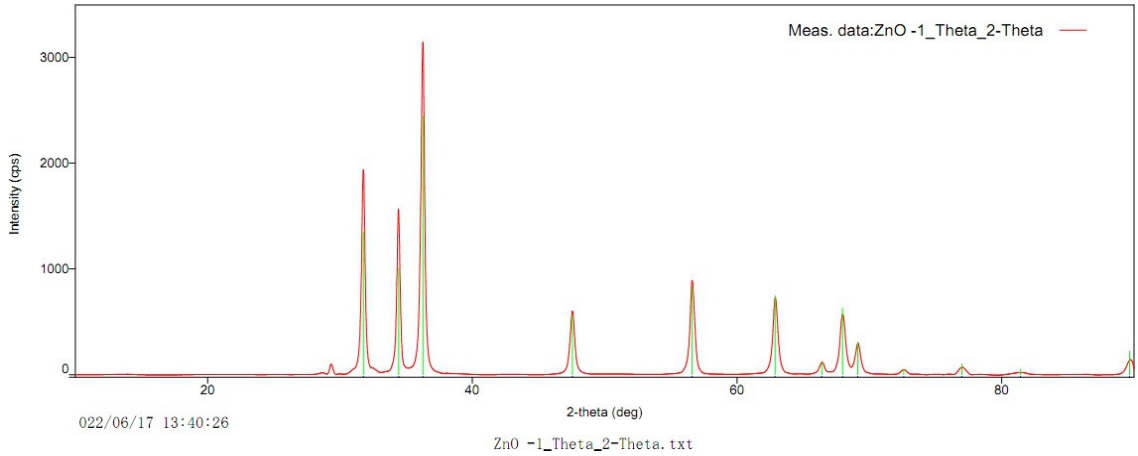

Fig. 2 XRD image of ZnO

XRD images of SnO_2-ZnO samples

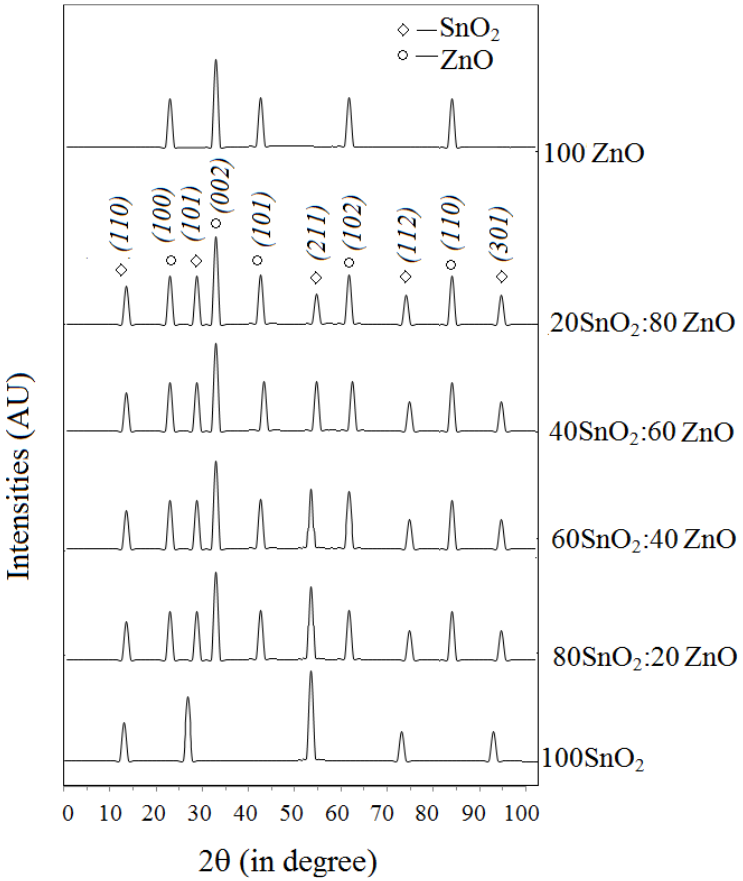

Fig. 3 XRD image of SnO_2+ ZnO composites

It is observed that as the mole % of ZnO in SnO_2 increases, the intensity of equivalent peak increases. ZnO (hexagonal) crystallizes in the wurtzite structure [4-6]. The lattice parameter values obtained for ZnO are a = b = 3.249 Å and c = 5.201 Å with c/a ratio of 1.6. The main peak of maximum intensity was found to be at 34.43° and corresponding to (0 0 2) plane. Others planes of ZnO are (1 0 0), (1 0 1), (1 0 2), (1 1 0). The crystallite size (D) was calculated from Scherer's formula using FWHM [9].

It was found that the $60SnO_2$:40ZnO sample had a lower average crystalline size, which translated into a larger active surface.

3.2 Scanning electron microscopy (SEM) Study

Because seeing is considered to be believed and understanding, for thin film and coating characterization the SEM (Scanning Electron Microscopy) is the most commonly used equipment. Zworykin first proposed the idea to image surface topography of materials by using

the secondary emission formed by a focused electron probe. SEM uses electron beam to scan the surface of a sample and produces images by knowing the electronic interactions with the sample interface [10].

The surface morphologies of PPy, Al_2O_3 SnO_2, ZnO, and their composites were studied by SEM and their photos are shown in the figures

From SEM Photos, it is observed that PPy is porous in nature and pore size varies from 25 to 80 nm. Due to small pores size, its surface area is more and it shows more active surface area. Some portion of SEM Photos shows rods with fine voids over them which helps to increase sensing properties [11].

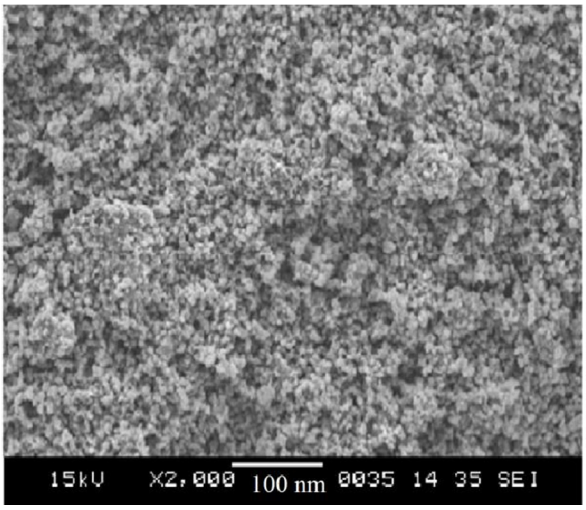

Fig. 4 SEM photo of PPy

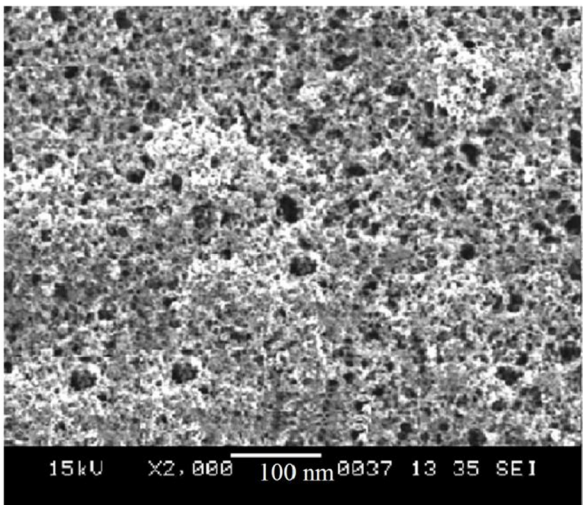

Fig. 5 SEM photo of SnO_2

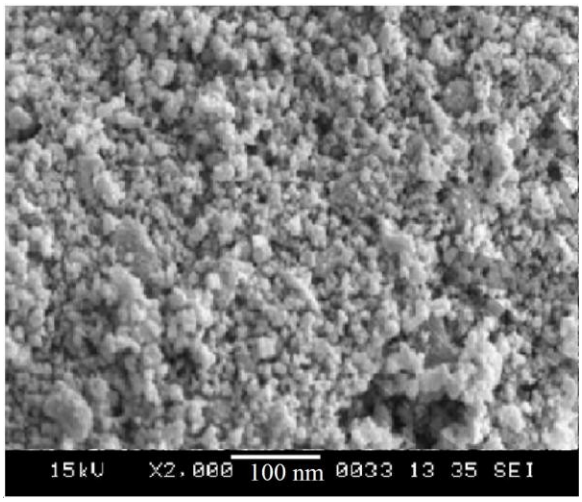

Fig. 6 SEM photo of ZnO

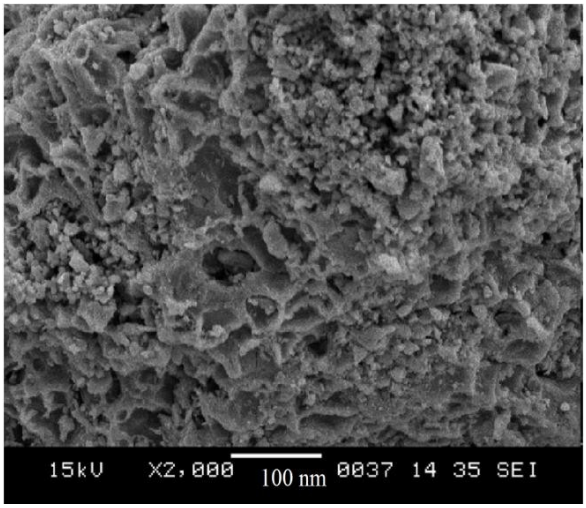

Fig. 7 SEM photo of $80SnO_2$:20ZnO

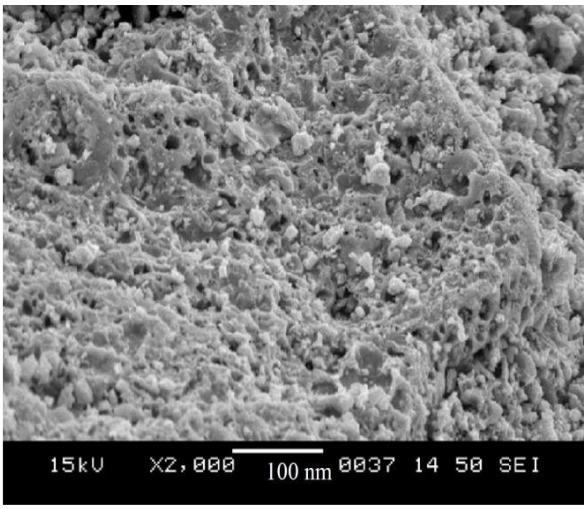

Fig. 8 SEM photo of $60SnO_2$:40ZnO

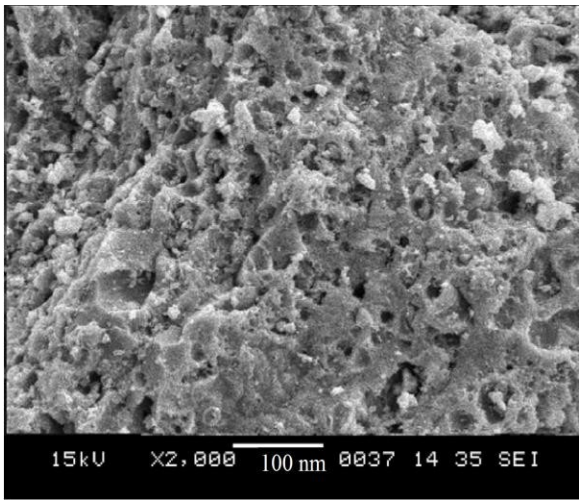

Fig 9 SEM photo of $40SnO_2$:60ZnO

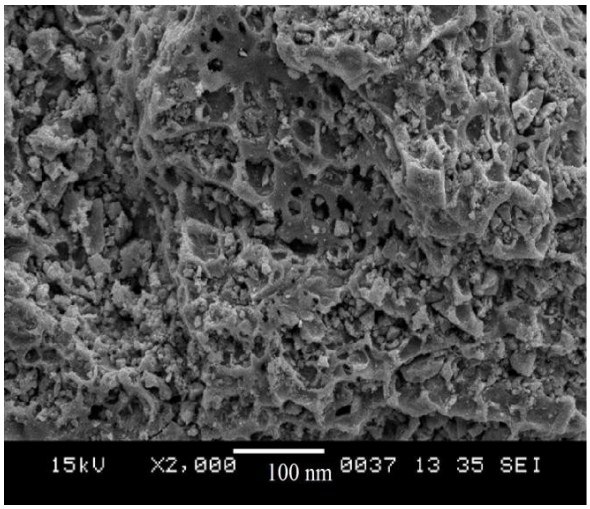

Fig10 SEM photo of $20SnO_2$:80ZnO

Table 2 Average number of pores of the samples measured per inch

Sr. No.	Pure sample and their compositions (mole %)	Number of pores per inch (in x 2000 magnification)
1.	PPy	118
2.	SnO_2	92
3.	ZnO	103
4.	$80SnO_2$:20 ZnO	123
5.	**$60SnO_2$:40 ZnO**	**132**
6.	**$40SnO_2$:60 ZnO**	**142**
7.	$20SnO_2$:80 ZnO	98

SEM photos reveled that out of PPy, SnO_2, ZnO, and PPy has more porosity. Out of different compositions of SnO_2 - ZnO and 40SnO2:60 ZnO compositions manifested enhanced porosity.

3.3 Resistance variations of sensors with CO_2 gas concentration

Resistance of the sensors is measured by using voltage drop method. A constant voltage source is used to apply constant voltage across the sensor in series with 10 Mega ohm resistances. Electric potential difference is measured across series resistance (10 MΩ) and from that, potential difference across sensor is calculated and hence resistance of the sensor can be determined. Measurement of sensor resistance is carried out at room temperature (300 k) and at step increase of temperature in the step of 30^0C each. Also, sensor air resistance is measured [12].

3.4 at room temperature 300 K, 330 K, 360 K

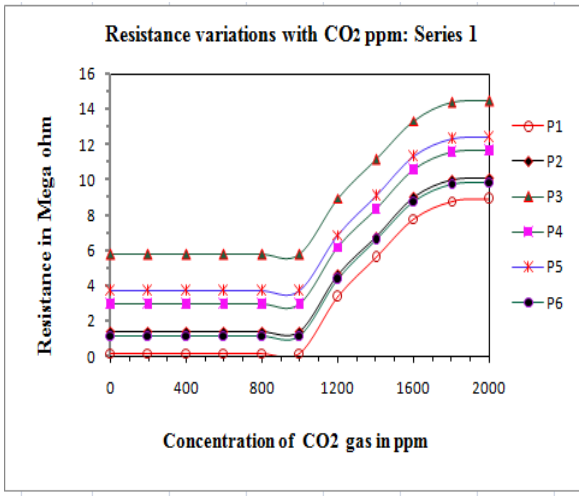

Fig. 11

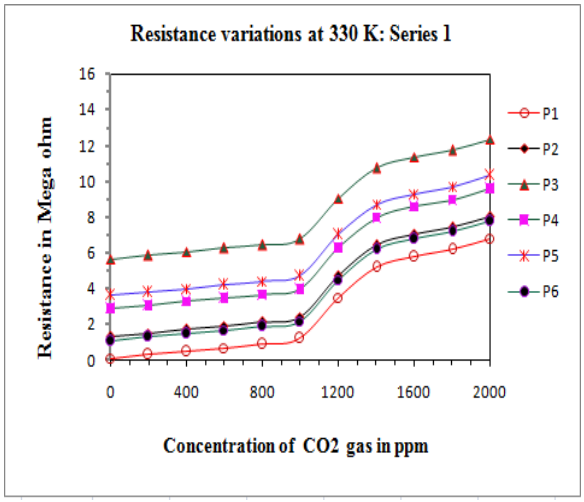

Fig. 12

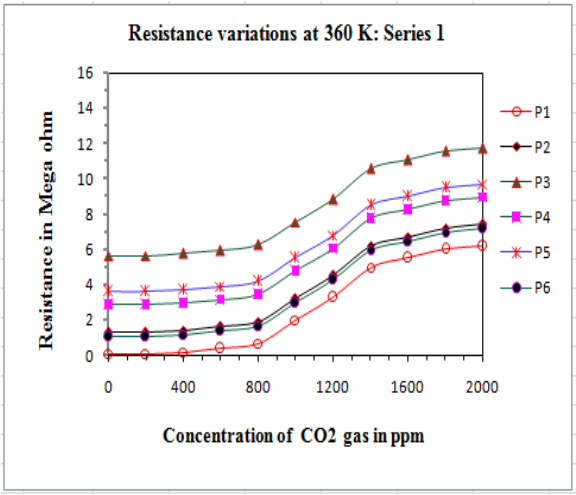

Fig. 13

3.5 CO_2 gas detection (Sensing) properties

Sensitivity or response of the sensors is measured in terms of change in resistance in the environment of CO_2 gas with respect to the resistance of the sensor in air surrounding.

Mathematically sensitivity is expressed as:

$$S = \left(\frac{R_g - R_a}{R_a} \right) = \left(\frac{\Delta R}{R_a} \right)$$

Where, R_g = sensor resistance in presence of gas

R_a = sensor resistance in the environment of air.

As the prepared sensors showed maximum variations in the resistance at room temperature i.e. 300 K, the sensivityvity was determined at room temperature. The variation of the sensitivity with respect to concentration of CO_2 gas at room tempeature in the form of line and bar graphs are shown in the following figures [13].

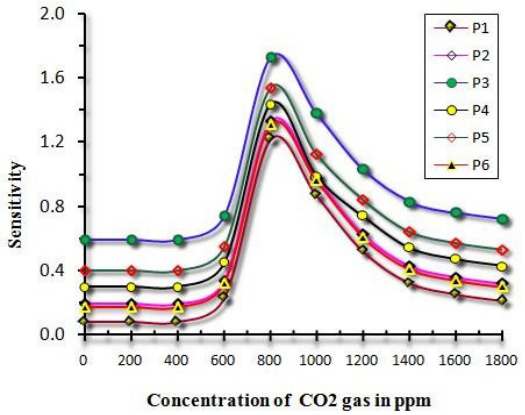

Fig. 14 Graph showing variation of sensitivity of P1 to P6 sensors at 300 K

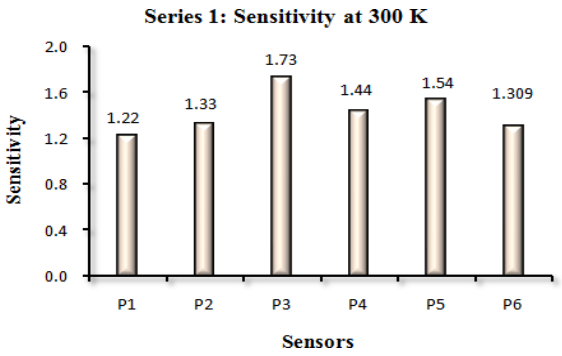

Fig. 15 Bar graph at 800 ppm of CO_2 gas showing high sensitivity of P3 sensor

3.6 Static Responses of optimize sensors

Static response curves for optimize sensors P3, Q4, R5 and S2 sensors at 600 ppm , 800 ppm and 1000 ppm of CO_2 gas concentration and at [14] room temperature (300 K) are shown in the following figure 16.

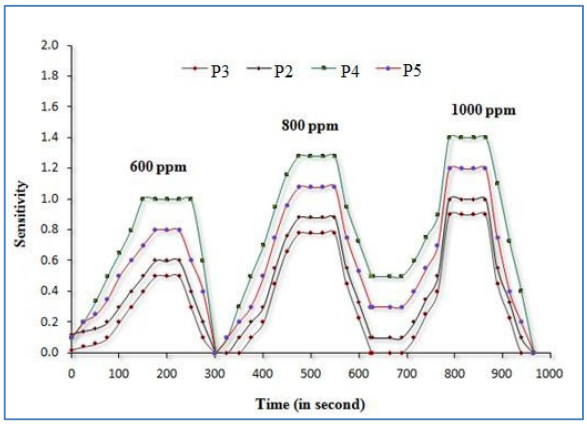

Fig. 16 Static response curves for optimize sensors P3, P2, P4, and P5 sensors

Static response curves of the optimize sensors exhibited response time and recovery time in second. For 800 ppm CO_2 gas concentration, these times are listed in following table 3.

Table 3 Response and Recovery times of optimize sensors

Sr. No.	Sample Compositions	Sensor	Response time (s) for 800 ppm	Recovery time (s) for 800 ppm
1	60SnO_2: 40ZnO/ PPy/GP	P3	151	58
2	80SnO_2: 20ZnO/ PPy/GP	P2	128	72

3	40SnO_2: 60ZnO/ PPy/GP	P4	99	45
4	20SnO_2: 80ZnO/ PPy/GP	P5	131	67

From table 3., it is observed that response time and recovery time of P4 sensors are found to be least and these are 99 s and 45 s respectively. This exhibits that P4 sensor is best among the prepared sensors from all the series [15].

3.7 Dynamic Responses of optimize sensors

The variation of sensitivity (dynamic response) of the prepared sensors was studied at 600, 800 and 1000 ppm as a function of time at room temperature (300 K) by exposing the CO_2 gas to the prepared sensors [16]. This response is shown in the following figure 17.

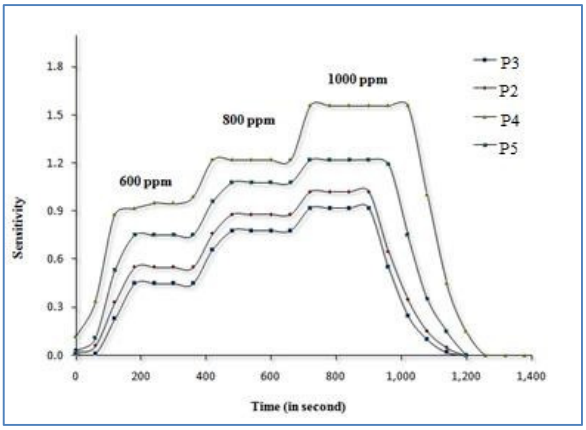

Fig. 17 Dynamic response curves for optimize sensors P3, P2, P4, and P5 sensors

Table 4 Recovery time of optimized sensors

Sr. No.	Sample Compositions	Sensors	Recovery time (s)
1	60SnO_2: 40ZnO/ PPy/GP	P3	225
2	80SnO_2: 20ZnO/ PPy/GP	P2	192
3	40SnO_2: 60ZnO/ PPy/GP	P4	136
4	20SnO_2: 80ZnO/ PPy/GP	P5	202

From table 4, P4 sensor observed to be having less recovery time (136 s) and hence this sensor found be faster in operation than other optimize sensors. This is because combination of 20SnO_2 and 80TiO_2 forms spongy surface and hence absorbs more gas and gave more response i.e. response time is less. Also PPy is more porous in nature and it's base to 20SnO_2: 80 TiO_2

supported in enhancing the response [17]. Reciprocal of recovery time is called fast response and it is shown in the following graph 18.

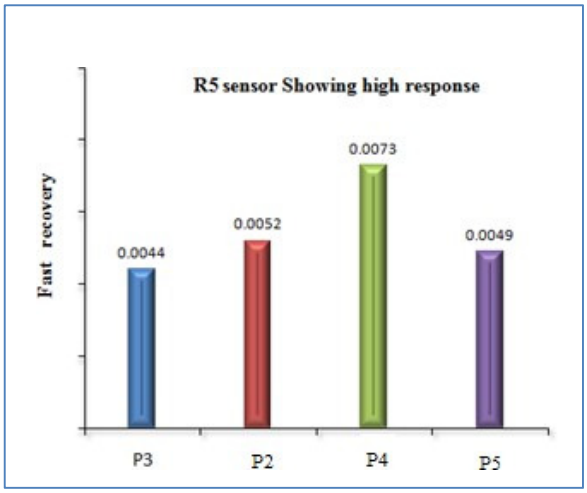

Fig. 18 R5 sensor showing high response at room temperature (300 K)

3.8 Stability of Sensors

Stability curves of optimized sensors P3, P2, P4 and P5 sensors at room temperature are shown in the following graph 19. Stability of the sensor is expressed in terms of resistance measurement with respect to time [18]. As time passes, change in resistance is measured and found to be nearly constant over longer time. This shows that sensor is most stable.

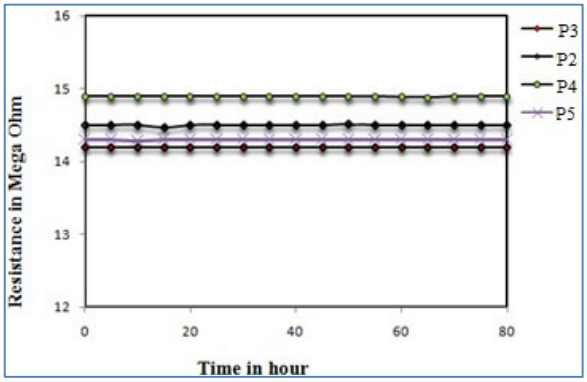

Fig.19. All optimized sensors found to be more stable with respect to time

3.9 Gas Selectivity of most optimized Sensor P3

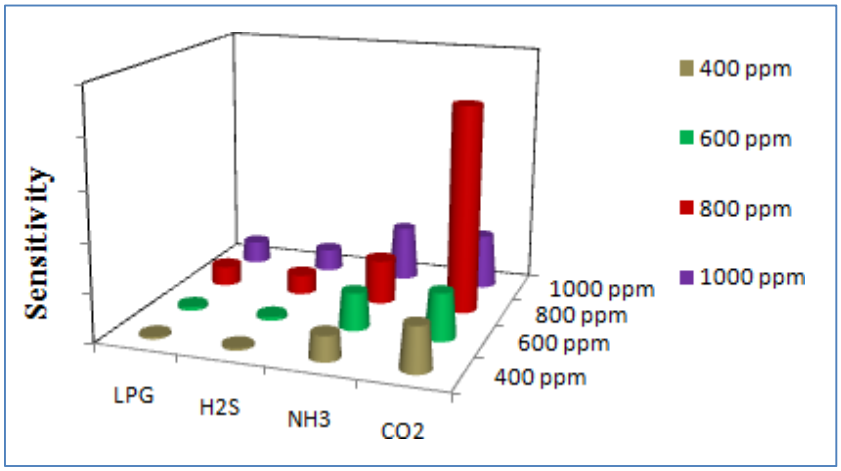

Fig.20. Selectivity Curve of Sensor P3

For checking the gas selectivity of P3 sensor, P3 sensor was exposed to various gases like CO_2, H_2S, LPG, and NH_3. The selectivity was selected for 400 ppm, 600 ppm, 800 ppm and 1000 ppm of all stated gas concentrations. The result exhibited that among all tested gases, for CO_2 gas at 800 ppm concentration P3 sensor showed enhanced response as compared to other gases at room temperature. Therefore this P3 sensor is best selective at room temperature and at 800 ppm CO_2 gas concentration. Thus P3 sensor can be used as hazardous gas sensing device in indoor and outdoor pollutant industries and places [19].

Conclusion

The study successfully synthesized and characterized semiconductor materials SnO_2, ZnO, and the conducting polymer PPy for CO_2 gas sensing. Key findings from this research include, Material Synthesis and Characterization**.** The synthesis of SnO_2 and ZnO nanoparticles, as well as the chemical polymerization of PPy, was achieved, with each material exhibiting distinctive structural and morphological properties. XRD analysis confirmed the formation of crystalline phases, with ZnO showing a hexagonal wurtzite structure. SEM revealed that PPy had a highly porous surface, which enhanced the gas adsorption capability. Gas-Sensing Performance the gas sensitivity of the sensors was evaluated by measuring changes in resistance when exposed to CO_2 at different concentrations. The P3 sensor, composed of 60% SnO_2 and 40% ZnO with PPy, showed the highest sensitivity to CO_2 at room temperature (300 K) compared to other compositions. It also exhibited fast response and recovery times, particularly at higher CO_2 concentrations (800 ppm), making it an ideal candidate for practical gas sensing applications.

Stability and Selectivity, the P3 sensor demonstrated excellent long-term stability with minimal resistance variation over time. Selectivity tests revealed that the P3 sensor was highly selective to CO_2, outperforming other gases like H_2S, LPG, and NH_3, which are often encountered in industrial environments. The SnO_2-ZnO-PPy composite sensors, especially the P3 variant, offer a promising solution for CO_2 detection, with high sensitivity, selectivity, and stability. These sensors can be effectively employed in environmental monitoring, industrial safety, and air quality control, where accurate CO_2 detection is essential. Future work will focus on optimizing these materials for other hazardous gases and enhancing the sensor's performance at higher operating temperatures.

Reference

[1] Fang Shimizu, Y.; Kai, S.; Takao, Y.; Hyodo, T.; Egashira, M. Correlation between methylmercaptan gas-sensing properties and its surface chemistry of SnO_2 based sensor materials. *Sens. Actuators B*, **2000**, *65*, 349-357.

[2] Bulpitt, C.; Tsang, S.C. Detection and differentiation of C-4 hydrocarbon isomers over the Pd-SnO_2 compressed powder sensor. *Sens. Actuators B*, **2000**, *69*, 100-107.

[3] Jenkins R, Snyder R L,. "Introduction to X-ray powder diffractometry", Wiley, New York, **1996**.

[4] Cullity B.D., "Elements of X-ray Diffraction ", Addison-Wesley Publishing Company Inc., London, **1978**.

[5] Kida, T.; Doi, T.; Shimanoe, K. Synthesis of monodispersed SnO_2 nanocrystals and their remarkably high sensitivity to volatile organic compounds. *Chem. Mater.,* **2010**, *22*, 2662-2667.

[6] Chen, T.; Mu, Q.Y.; Zhou, Z.L.; Wang, Y.D. Synthesis and formaldehyde sensing properties of Pd-doped SnO_2 nanoparticles. *Sens. Lett.*, **2010**, *8*, 238-242.

[7] Huang, J.R.; Wang, J.H.; Zhukova, A.A.; Rumyantseva, M.N.; Gaskov, A.M.; Yu, K.; Gu, C.P.; Liu, J.H. High-sensitivity humidity sensor based on a single Sb-doped SnO_2 whisker. *Sens. Lett.*, **2009**, *7*, 1025-1029.

[8] Yoo, K.S.; Park, S.H.; Kang, J.H. Nano-grained thin-film indium tin oxide gas sensors for H_2 detection. Sens. Actuators B, **2005**, 108, 159-164.

[9] Yang, Y.; Kim, D.-H.; Kim, W.-S.; Kang, T.J.; Lee, B.Y.; Hong, S.; Kim, Y.H.; Hong, S.-H. H_2 sensing characteristics of SnO_2 coated single wall carbon nanotube network sensors. Nanotechnology, **2010**, 21, 215501.

[10] Gao, T.; Wang, T.H. Sonochemical synthesis of SnO_2 nanobelt/CdS nanoparticle core/shell heterostructures. Chem. Commun., **2004**, 22, 2558-2559.

[11] Han, X.M.; Zhang, B.; Guan, S.K.; Liu, J.D.; Zhang, X.; Chen, R.F. Gassensing properties of SnO_2 nanobelts synthesized by thermal evaporation of Sn foil. J. Alloys Comp., **2008**, 461, L26-L28.

[12] Kumar, S.; Peng, Z.C.; Shin, H.; wang, Z.L.; Hesketh, P.J. AC dielectrophoresis of tin oxide nanobelts suspended in ethanol: manipulation and visualization. Anal. Chem., **2010**, 82, 2204-2212.

[13] Huang, H.; Lee, Y.C.; Tan, O.K.; Zhou, W.; Peng, N.; Zhang, Q. High sensitivity SnO_2 single-nanorod sensors for the detection of H_2 gas at low temperature. Nanotechnology, **2009**, 20, 115501.

[14] Huang, J.; Matsunaga, N.; Shimanoe, K.; Yamazoe, N.; Kunitake, T. Nanotubular SnO_2 templated by cellulose fibers: Synthesis and gas sensing. Chem. Mater., **2005**, 17, 3513-3518.

[15] Huang, H.; Lee, Y.C.; Chow, C.L.; Tan, O.K.; Tse, M.S.; Guo, J.; White, T. Plasma treatment of SnO_2 nanocolumn arrays deposited by liquid injection plasma-enhanced chemical vapour deposition for gas sensors. Sens. Actuators B, **2009**, 138, 201-206.

[16] Du, N.; Zhang, H.; Ma, X.Y.; Yang, D.R. Homogeneous coating of Au and SnO_2 nanocrystals on carbon nanotubes via layer-by-layer assembly: a new ternary hybrid for a room-temperature CO gas sensor. Chem. Commun., **2008**, 46, 6182-6184.

[17] Fields, L.L.; Zheng, J.P.; Cheng, Y.; Xiong, P. Room-temperature low-power hydrogen sensor based on a single tin dioxide nanobelt. Appl. Phys. Lett., **2006**, 88, 263102.

[18] Comini, E.; Faglia, G.; Sberveglieri, G.; Pan, Z.W.; Wang, Z.L. Stable and highly sensitive gas sensors based on semiconducting oxide nanobelts. Appl. Phys. Lett., **2002**, 81, 1869-1871.

[19] Comini, E.; Faglia, G.; Sberveglieri, G.; Calestani, D.; Zanotti, L.; Zha, M. Tin oxide nanobelts electrical and sensing properties. Sens. Actuators B, **2005**, 111, 2-6.